Frequency-Dependent Low Order Approximation of Transmission Line Parameters

Alécio B. Fernandes
alecio@dee.ufpb.br

Washington L. A. Neves
waneves@dee.ufpb.br

Universidade Federal da Paraíba (UFPB)
Departamento de Engenharia Elétrica
Av. Aprígio Veloso, 882
58.109-970 - Campina Grande - PB – Brazil

Abstract - **In EMTP-type programs, the J. Martí's frequency-dependent transmission line model (fdline) is largely used. In this model, multiphase lines are decoupled through modal transformation matrices. The characteristic admittance $Y_c(\omega)$ and the propagation function $A(\omega)$ are approximated by rational functions using the asymptotic fitting technique. However, the approximated functions usually have a high number of zeroes and poles, and may produce large local errors. In this paper, an optimization fitting procedure is used to obtain low order approximation for $Y_c(\omega)$ and $A(\omega)$ to be used in connection with the J. Martí's model. The approximated functions are obtained for three and six-phase line configurations. Time-domain digital simulations were carried out. It is shown that the low order model may produce more accurate results than those obtained by some currently available EMTP routines. Computer time savings are also accomplished.**

Keywords: EMTP, Line modelling, Optimization, Low Order Model, Real-Time Simulators.

I. INTRODUCTION

The frequency range associated with a transient condition, in power systems, can vary from 0,1 Hz up to 50 MHz [1]. In this frequency range, the transmission line parameters are strongly frequency dependent, due to ground return, skin effect and multiphase coupling.

J. Marti's transmission line model (fdline) is largely used in EMTP-type programs [2]. In fdline model, multiphase lines are decoupled through modal transformation matrices, based on Wedepohl and Hedman's theory of decomposition of natural propagation modes (eigenmodes) [3,4]. In the frequency domain, each mode of the transmission line is represented by the characteristic admittance, $Y_c(\omega)$, in parallel with a current source (Fig. 1). The current source is a function of the propagation function, $A(\omega)$.

J. Martí suggests an alternative form for frequency-time conversion which avoids inverse transformations (Fourier Transform, for example). $Y_c(\omega)$ and $A(\omega)$ are approximated by rational functions using the asymptotic fitting technique. However, the approximated functions usually have a high number of zeroes and poles, and may produce large local errors when comparated to the original characteristic admittance and propagation function curves [5, 6].

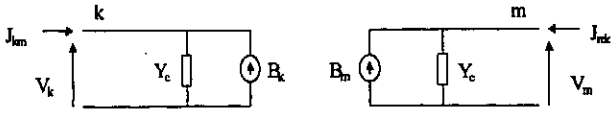

Fig. 1. Transmission line equivalent circuit in modal domain.

Low order approximate functions may be important for real time studies. Some authors show that the use of low order functions provides a reduction in the processing time in each time step [7, 8, 9]. Simulations in real time are then accomplished, although large errors had to be accepted in the fitting process.

This work is based on the optimization fitting procedure presented previouly by the authors [6]. With this procedure, accurate low order models are obtained. Digital simulations are carried out using MICROTRAN® [10] and ATP [11]. The differences in the simulated results are analyzed. Low order models lead to smaller processing time per time step.

II. TIME-DOMAIN MODEL

The frequency domain equivalent circuit of a transmission line is shown in Fig. 1, where:

$$\begin{aligned} B_k(\omega) &= \left[Y_c(\omega)V_m(\omega) + J_{mk}(\omega)\right].A(\omega) \\ B_m(\omega) &= \left[Y_c(\omega)V_k(\omega) + J_{km}(\omega)\right].A(\omega). \end{aligned} \tag{1}$$

In the time-domain,

$$\begin{aligned} b_k(t) &= \left[y_c(t) * v_m(t) + j_{mk}(t)\right] * a(t) \\ b_m(t) &= \left[y_c(t) * v_k(t) + j_{km}(t)\right] * a(t). \end{aligned} \tag{2}$$

In (2) the symbol "*" denotes convolution integrals.

For time-domain simulations, $Y_c(\omega)$ is approximated by $Y_{eq}(\omega)$ in rational function form (with $s=j\omega$):

$$Y_{eq}(s) = \frac{N(s)}{D(s)} = H \cdot \frac{(s+z_1).(s+z_2).....(s+z_n)}{(s+p_1).(s+p_2).....(s+p_n)}, \tag{3}$$

that can be rewritten in partial fraction form,

$$Y_{eq}(s) = k_\infty + \frac{k_1}{(s+p_1)} + \frac{k_2}{(s+p_2)} + \cdots + \frac{k_n}{(s+p_n)}. \tag{4}$$

Using a numerical integration method, each terminal of Fig. 1 can be reduced to the equivalent circuit of Fig. 2, in which the frequency-dependent line admittance is

represented by a constant admittance, Y_{eq}, in parallel with a current source, $J_{k\text{-}eq}(t)$.

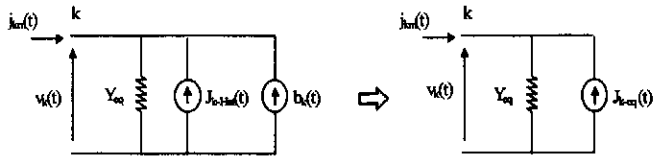

Fig. 2. Time-domain equivalent circuit.

In Fig. 2, $J_{k\text{-}eq}(t) = b_k(t) + J_{k\text{-}Hist}(t)$.

In (2),

$$b_k(t) = \left[y_c(t) * v_m(t) + j_{mk}(t)\right] * a(t) .$$

Thus, from the circuit of Fig. 2,

$$b_k(t) = \left[Y_{eq} . v_m(t) + j_{mk}(t) + J_{m-Hist}(t)\right] * a(t) - J_{k-Hist}(t) . \quad (5)$$

Or further,

$$b_k(t) = f_m(t) * a(t) - J_{k-Hist}(t) , \quad (6)$$

where: $f_m(t) = Y_{eq} \cdot v_m(t) + j_{mk}(t) + J_{m-Hist}(t)$;

$a(t) = \mathcal{F}^{-1}\{A(\omega)\}$ = Inverse transform of $A(\omega)$.

Therefore, to determine $b_k(t)$, we need to obtain $a(t)$. $A(\omega)$ is approximated by a rational function:

$$A_{eq}(s) = P(s) . e^{-s.\tau_{min}} \text{ (with } s = j\omega), \quad (7)$$

where: τ_{min} = travel time of the fastest wave; and

$$P(s) = \frac{N(s)}{D(s)} = H . \frac{(s+z_1).(s+z_2).....(s+z_n)}{(s+p_1).(s+p_2).....(s+p_m)} . \quad (8)$$

Thus, $P(s)$ can be written in the form,

$$P(s) = \left\{ \frac{k_1}{s+p_1} + \frac{k_2}{s+p_2} + \cdots + \frac{k_m}{s+p_m} \right\} . \quad (9)$$

Returning to the time-domain,

$$p(t) = \left\{ k_1 . e^{-p_1 t} + k_2 . e^{-p_2 t} + ...+ k_m . e^{-p_m t} \right\} . \quad (10)$$

Using (10) and (7) the convolution integral (6) can be evaluated recursively at each time step [2, 5].

III. THE FITTING TECHNIQUES

EMTP programs, like MICROTRAN® and ATP use the well known asymptotic fitting technique based on Bode's procedure to approximate the characteristic admittance (or impedance) and propagation function [2].

The optimized fitting technique used here was first presented in [6]. It is based on an optimization procedure due to Levenberg-Marquardt [12]. Low order approximated functions can be obtained with good accuracy in all frequency range. The number of poles and zeroes is defined by the user for each mode.

IV. CASE STUDIES

In this section, three different case studies using both, the asymptotic and optimized fitting procedures, are analyzed.

CASE A:

Consider the three-phase untransposed overhead transmission line with ground wires as shown in Fig. 3.

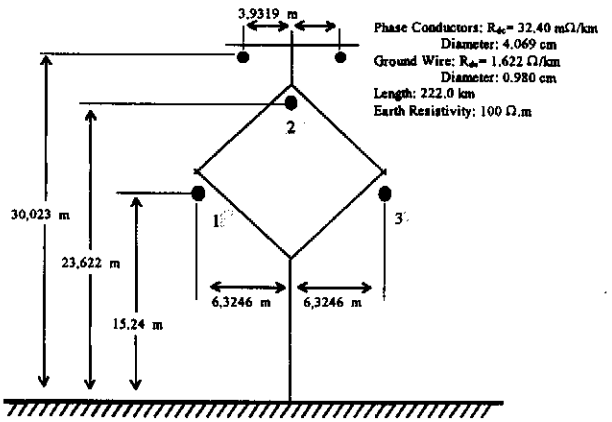

Fig. 3. Untransposed three-phase transmission line with explicit ground wires.

Using FDDATA™ (MICROTRAN® Student Version 2.08), the 05 modes (three phases and two ground wires) of $Y_c(\omega)$ and $A(\omega)$ were computed for a frequency range from 10^{-2} Hz to 10^6 Hz. The asymptotic fitting technique and the optimized fitting procedure were used to find the rational function approximations for $Y_c(\omega)$ and $A(\omega)$. The fitting results are shown in Fig. 4 to 7 and summarized in Table 1. In general, the maximum error occurs in the low frequency range for $Y_c(\omega)$, and in the high frequency range for $A(\omega)$.

Table 1 - Comparison between the two fitting procedures Case A.

		Asymptotic Fitting			Optimized Fitting		
	Mode	zero	pole	Max. Error (%)	zero	pole	Max. Error (%)
$Y_c(\omega)$	01	10	10	35,38	05	05	2,81
	02	14	14	10,33	05	05	1,06
	03	07	07	9,55	05	05	1,04
	04	18	18	9,14	08	08	0,71
	05	21	21	6,63	09	09	0,16
$A(\omega)$	01	18	20	3,07	06	09	0,31
	02	19	20	8,96	07	09	0,14
	03	16	18	7,08	07	11	4,56
	04	22	24	6,62	03	06	1,63
	05	18	20	5,65	06	08	5,13

It can be seen that if the optimized fitting procedure is used, a low order rational function is obtained with very good accuracy over the entire frequency range.

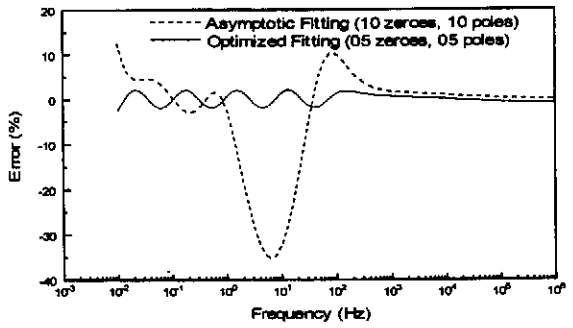

Fig. 4. Admittance Error Curves
Magnitude of Mode 01.

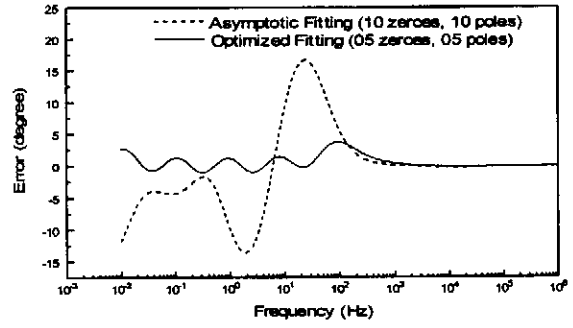

Fig. 5. Admittance Error Curves
Phase of Mode 01.

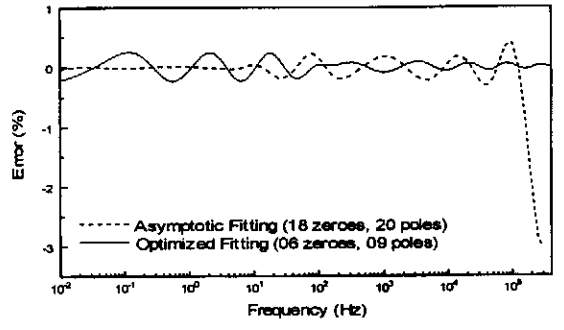

Fig. 6. Propagation Function Error Curves
Magnitude of Mode 01.

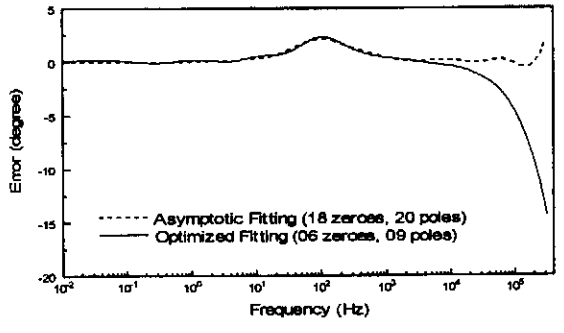

Fig. 7. Propagation Function Error Curves
Phase of Mode 01.

MICROTRAN® was used to carry out time-domain simulations. A voltage step was applied to phase 1 at the sending end with the receiving end and the other phases left opened. A time step of $\Delta t = 1\mu s$ and the modal transformation matrix, calculated at *1,2 kHz* from FDDATA™, were used. The simulated results are shown in Fig. 8 and Fig. 9. In Fig. 8 three curves are plotted. Note that the FDDATA model curve and the low order model curve are nearly identical. A FFT (Fast Fourier Transform) program was used to obtain the frequency spectrum for each voltage waveform at the receiving end (Fig. 10 and Fig. 11). Only the lower frequency range of the spectrum is shown for in the upper part of the spectrum it does not appear any discrepancy between frequency components.

In the low frequency range, discrepancies are observed. In this frequency range, the error in the approximated admittance produced by the asymptotic fitting procedure is maximum for all admittance modes (Table 1).

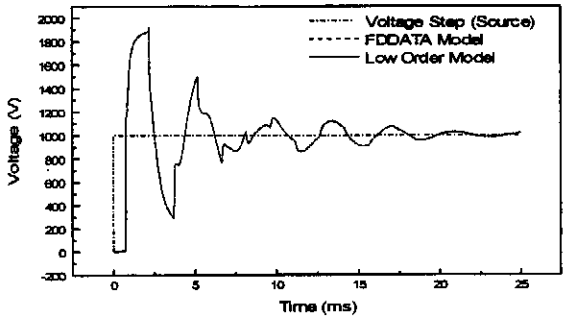

Fig. 8. Voltage at the receiving end - Phase 1.

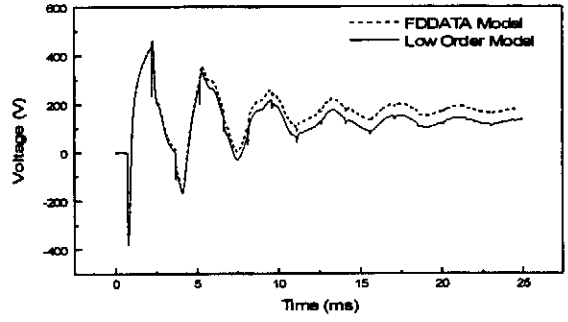

Fig. 9. Voltage at the receiving end - Phase 2.

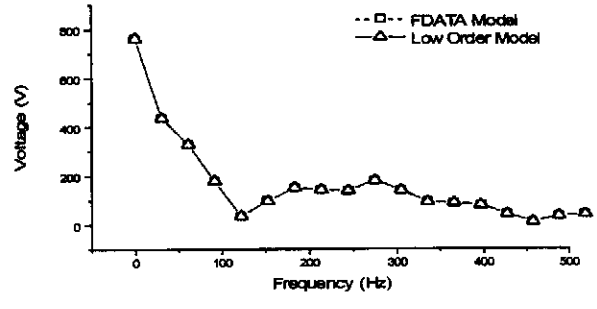

Fig. 10. Low frequencies (0-500 Hz) FFT Magnitude Plot of voltage at receiving end - Phase 1.

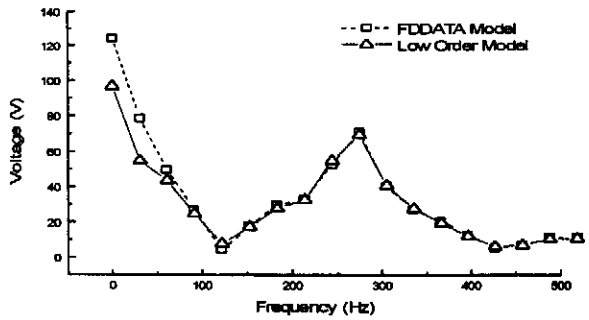

Fig. 11. Low frequencies (0-500 Hz) FFT Magnitude Plot of voltage at receiving end - Phase 2.

CASE B:

Consider the three-phase untransposed overhead transmission line of Fig. 12.

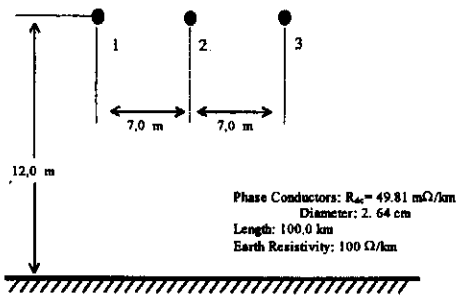

Fig. 12. Untransposed three-phase transmission line.

Using FDDATA™, the 03 modes of $Y_c(\omega)$ and $A(\omega)$ were computed for the frequency range from 10^{-2} Hz to 10^6 Hz. The asymptotic fitting technique and the optimized fitting procedure were used to find the rational function approximations for $Y_c(\omega)$ and $A(\omega)$. The fitting results are summarized in Table 2. Again, the maximum errors occur in the low frequency range for characteristic admittance and in the high frequency range for propagation function. The optimized fitting procedure produces a very low order rational function with a very small maximum error, over the entire frequency range.

MICROTRAN® was used to carry out time-domain with a time step of $\Delta t = 1\,\mu s$. A voltage step was applied to phase 1 at the sending end with the receiving end and the other phases left opened. The simulated results are shown in Fig. 13.

The FFT (Fast Fourier Transform) program was used to obtain the frequency spectrum for each voltage waveform at the sending end (Fig. 14). Again, only the lower frequency range of the spectrum is shown. In the upper part of the spectrum the discrepancies are negligible. The discrepancies in the low frequency range are due to errors in the approximated admittance produced by the asymptotic fitting procedure for all modes (Table 2).

Table 2 -Comparison between the two fitting procedures Case B.

		Asymptotic Fitting			Optimized Fitting		
	Mode	zero	pole	Max. Error (%)	zero	pole	Max. Error (%)
$Y_c(\omega)$	01	20	20	9.52	08	08	0.94
	02	14	14	10.13	05	05	1.51
	03	14	14	10.30	05	05	1.35
$A(\omega)$	01	20	22	17.71	02	05	4.64
	02	18	19	3.88	02	03	1.36
	03	20	22	16.85	02	05	3.08

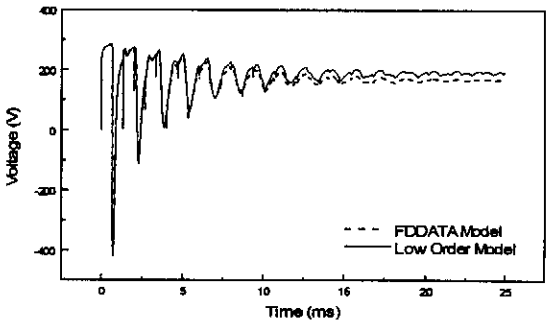

Fig. 13. Voltage at sending end - Phase 2.

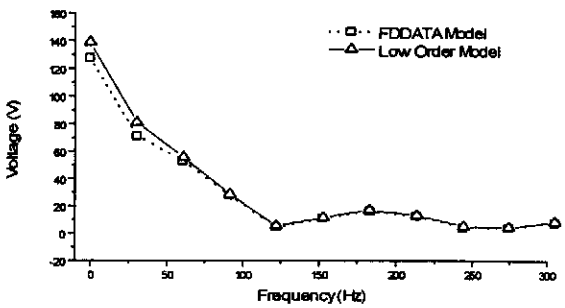

Fig. 14. Low frequencies (0-300 Hz) FFT magnitude plot of voltage at sending end - Phase 2.

CASE C:

Consider the double circuit three-phase untransposed overhead transmission line of Fig. 15.

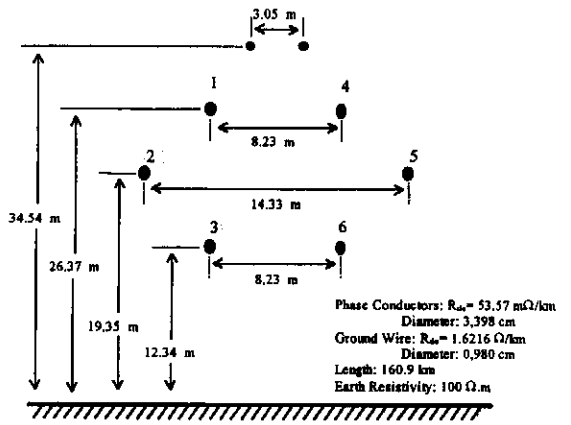

Fig. 15. Double untransposed three-phase transmission line.

Using LINE CONSTANTS routine (ATP), the 06 modes of $Z_c(\omega)$ and $A(\omega)$ were computed for a frequency range from 10^{-1} Hz to 10^6 Hz. The asymptotic fitting technique and the optimized fitting procedure were used to find the rational function approximations for $Z_c(\omega)$ and $A(\omega)$. The fitting results for the 06 modes are summarized in Table 3.

Table 3 – Comparison between the two fitting procedures Case C.

		Asymptotic Fitting			Optimized Fitting		
	Mode	zero	pole	Max. Error (%)	zero	pole	Max. Error (%)
$Z_c(\omega)$	01	24	24	8.92	07	07	0.87
	02	25	25	9.68	07	07	0.13
	03	25	25	9.66	07	07	0.16
	04	17	17	9.69	07	07	0.17
	05	23	23	9,70	07	07	0.18
	06	24	24	9.63	07	07	0.15
$A(\omega)$	01	15	18	4.86	08	11	1.46
	02	15	17	2.03	10	12	0.84
	03	35	37	1.55	10	12	0.28
	04	21	22	1.18	07	08	0.48
	05	24	25	2.45	07	08	0.30
	06	24	25	3.01	07	08	0.10

Again, the maximum errors occur in low frequency range for characteristic admittance, and in high frequency range for propagation function. It can be seen that if the optimized fitting procedure is used, a low order rational function is obtained with a small maximum error, over the entire frequency range.

ATP was used to carry out time-domain simulations using models obtained with the asymptotic and the optimized fitting procedures. A voltage step was applied to phase 1, 2 and 3 at the sending end with the receiving end grounded and the other phases closed to ground by a 10Ω resistor. A time step $\Delta t = 5\mu s$ and the modal transformation matrix, calculated *1,2 kHz* from LINE CONSTANTS routine, were used. The simulated currents at the receiving end are shown in Fig. 16.

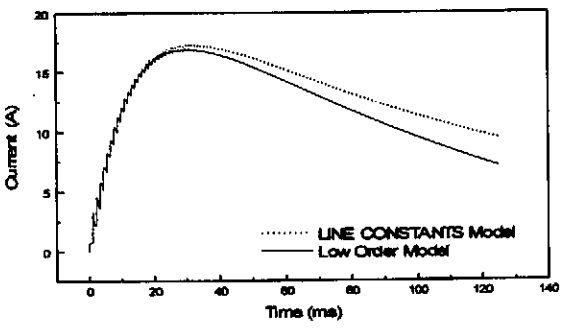

Fig. 16. Current in receiving end at Phase 6.

The FFT (Fast Fourier Transform) was applied to the current waveforms. Fig. 17 shows low frequencies (0-100Hz) FFT magnitude plots. Once more, it can be seen that discrepancies appear in the lower frequency components.

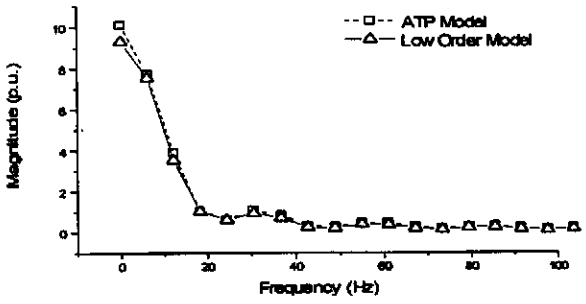

Fig. 17. Low frequencies (0-100 Hz) FFT magnitude plot of current in receiving end - Phase 6.

V. PROCESSING TIME

The simulations were performed with a PENTIUM® II 400 MHz, 128 MB - RAM. The elapsed time per time step for Case A, B and C are shown in tables 4, 5, and 6, respectively.

The use of low order functions provided a reduction in the processing time in each time step. The computer time savings were around 12% for cases A and B, and 22% for case C. In spite of the small time reduction (32 up to 80 μs), it may be important in real-time simulations.

Table 4 – Simulation time per number of time steps Case A - MICROTRAN®.

FDDATA™ Model (Asymptotic Fitting)	Low Order Model (Optimized Fitting)
9.8 / 25000 = 392 μs	8.6 / 25000 = 344 μs

Table 5 – Simulation time per number of time steps Case B - MICROTRAN®.

FDDATA™ Model (Asymptotic Fitting)	Low Order Model (Optimized Fitting)
6.6 / 25000 = 264 μs	5.8 / 25000 = 232 μs

Table 6 – Simulation time per number of time steps Case C - ATP.

LINE CONSTANTS Model (Asymptotic Fitting)	Low Order Model (Optimized Fitting)
9.0 / 25000 = 360 μs	7.0 / 25000 = 280 μs

VI. CONCLUSIONS

An optimization procedure to fit rational functions to $Z_c(\omega)$ and $A(\omega)$, was used. It was shown that the number of poles and zeroes of the fitted function can be considerably smaller than those obtained by using the asymptotic procedure, over the entire frequency range with good accuracy. Simulations were performed for three and six phase overhead lines.

FDDATA™ and LINE CONSTANTS fitting routines results may present large local errors, due to the asymptotic fitting procedure. The fitting process may lead to inaccurate results in time domain simulations.

The optimized fitting procedure used here may lead to more accurate results in time-domain simulations. In our studies, we have no problems with stability of the solution.

Recently, phase-domain models have been used [13-16]. In these models $Z_c(\omega)$ and $A(\omega)$ are fitted directly in phase-domain, avoiding modal transformations. The optimized routine presented here may be used in connection with these models.

Due to the accuracy and low order of approximated fitted functions, the optimized routine may be suitable to be used in connection with real-time simulators.

VII. ACKNOWLEGMENTS

The authors would like to thank the reviewers for their valuable suggestions. The financial support of Mr. Alécio Fernandes from the Brazilian National Research Council (CNPq) is gratefully acknowledged.

VIII. REFERENCES

[1] Cigré Working Group 33.02, "Guidelines for Representation of Network Elements when Calculating Transients", *Technical Brochure CE/SC GT/WG 02*, 1990.

[2] J. R. Martí, "Accurate Modelling of Frequency-Dependent Transmission Lines in Electromagnetic Transients Simulations", *IEEE Trans. Power Apparatus and Systems*, Vol. PAS-101, No. 1, pp. 147-157, January, 1982.

[3] L. M. Wedepohl, "Application of Matrix Methods to the Solution of Travelling-Wave Phenomena in Polyphase Systems", *Proc. IEE*, Vol. 110, n°12, pp. 2200-2212, December, 1963.

[4] D. E. Hedman, "Propagation on Overhead Transmission Lines. I - Theory of Modal Analysis. II - Earth-Conduction Effects and Practical Results", *IEEE Trans. on Power Apparatus and Systems*, Vol. PAS-84, pp. 205-211, May, 1965.

[5] H. W. Dommel, "Electromagnetic Transients Program Reference Manual", *Department of Electrical Engineering - The University of British Columbia*, Vancouver, 1996.

[6] A. B. Fernandes, W. L. A. Neves, "Transmission Lines: Fitting Technique Optimization", *Proceedings of the 1997 International Conference on Power Systems Transients*, Seattle, USA, June 22-26, 1997.

[7] X. Wang, R. M. Mathur, "Real-Time Digital Simulator of The Electromagnetic Transients of Transmission Lines with Frequency Dependence", *IEEE Trans. on Power Delivery*, Vol. 4, No. 4, pp. 2249-2255, October, 1989.

[8] C. Dufour, H. Le-Huy, J.C. Soumagne,, A. Hakimi, "Real-Time Simulation of Power Transmission Lines Using Marti Model With Optimal Fitting on Dual-DSP Card", *IEEE Trans. on Power Delivery*, Vol. 11, No. 1, January 1996.

[9] J. Sousa, M.T. Correia de Barros, O. Huet, "Frequency-Dependent Transmission Line Modelling for a Real-Time Digital Simulator", *Proceedings of the 1997 International Conference on Power Systems Transients*, pp. 460-465, Seattle, USA, June 22-26, 1997.

[10] Microtran Power System Analysis Corporation, "Transients Analysis Program Reference Manual", Vancouver, 1992.

[11] Leuven EMTP Center, "ATP - Alternative Transient Program - Rule Book", Herverlee, Belgium, July, 1987.

[12] W. H. Press, S. A. Teukolsky, W. T. Vetterling, B. P. Flannery, *Numerical Recipes in Fortran - The Art of Scientific Computing*, Second Edition, New York, Cambridge University Press, 1992.

[13] F. J. Marcano, J. R. Martí, "Idempotent Line Model: Case Studies" *Proceedings of the 1997 International Conference on Power Systems Transients*, pp. 67-72, Seattle, USA, June 22-26, 1997.

[14] F. Castellanos, J. R. Martí, F. Marcano, "Phase-Domain Multiphase Transmission Line Models", *Electrical Power & Energy Systems*, Vol. 19, No. 4, pp. 241-248, Elsevier Science Ltd., 1997.

[15] A. Morched, B. Gustavsen, M. Tartibi, "A Universal Model for Accurate Calculation of Electromagnetic Transients on Overhead Lines and Underground Cables", *IEEE Summer Meeting*, PE-112, PWRD-0-11-1997.

[16] Angelidis, G., Semlyen, A., "Direct Phase-Domain Calculation of Transmission Line Transients using Two-Sided Recursions", *IEEE Trans. on Power Delivery*, Vol. 10, No. 2, pp. 941-949, April, 1995.